Delineation of the central melanocortin circuitry controlling the kidneys by a virally mediated transsynaptic tracing study in transgenic mouse model

Tao Tao Liu[1], Bao Wen Liu[1], Zhi Gang He[1], Li Feng[1], San Guang Liu[2] and Hong Bing Xiang[1]

[1] Department of Anesthesiology and Pain Medicine, Tongji Hospital of Tongji Medical College, Huazhong University of Science and Technology, Wuhan, Hubei, People's Republic of China

[2] Department of Hepatobiliary Surgery, The Second Hospital, Hebei Medical University, Shijiazhuang, People's Republic of China

Correspondence to: San Guang Liu, *email*: sanguang1998@sina.com

ABSTRACT

To examine if brain neurons involved in the efferent control of the kidneys possess melanocortin-4 receptor (MC4-R) and/or tryptophan hydroxylase (TPH). Retrograde tracing pseudorabies virus (PRV)-614 was injected into the kidneys in adult male MC4R-green fluorescent protein (GFP) transgenic mice. After a survival time of 3-7 days, spinal cord and brain were removed and sectioned, and processed for PRV-614 visualization. The neurochemical phenotype of PRV-614-positive neurons was identified using double or triple immunocytochemical labeling against PRV-614, MC4R, or TPH. Double and triple labeling was quantified using microscopy. The majority of PRV-614 immunopositive neurons which also expressed immunoreactivity for MC4R were located in the ipsilateral intermediolateral cell column (IML) of the thoracic spinal cord, the paraventricular nucleus (PVN) of the hypothalamus, and raphe pallidus (RPa), nucleus raphe magnus (NRM) and ventromedial medulla (VMM) of the brainstem. Triple-labeled MC4R/PRV-614/TPH neurons were concentrated in the PVN, RPa, NRM and VMM. These data strongly suggest that central MC4R and TPH are involved in the efferent neuronal control of the kidneys.

INTRODUCTION

As an important determinant of balancing the volume and composition of body fluids, the kidneys play a critical role in the homeostatic control of water and sodium [1-3], and understanding the mechanisms of their central control could lead to pharmacological and behavioral therapeutic tools of renal-related disease, e.g. renal hypertension and renal diabetes. It is clear that kidneys are received from the body in the form of circulating hormones (arginine vasopressin (AVP), angiotensin AT1, etc.) [4-7], fuels (glucose, etc.) [8, 9], and other factors from the internal or external stimuli (chronic cold exposure, plasma volume expansion, etc.) [10, 11]. Activation of renal sympathetic nerves produces marked changes in renal hemodynamics, tubular ion, water transport and renin secretion [12, 13]. In addition, many other sensory, metabolic, and emotional factors also influence renal sympathetic activity or induce the change of renal function, suggesting that between brain and kidneys comprise a complex neural circuit that integrates multiple signals relevant for this change.

A large number of significant scientific reports demonstrated that the melanocortinergic signaling pathway constitutes a major signaling system in the control of energy homeostasis [14-27]. It has been evidenced that the central melanocortin system plays an important role in the regulation of basal plasma insulin levels and glucose tolerance [28-32]. A growing body of literature supports that sympathetic activity are tightly interconnected *via* hypothalamic melanocortinergic pathways involving the melanocortin-4 receptor (MC4R), a G protein-coupled, seven-transmembrane receptor expressed in the brain [15, 33-35]. MC4R-knockout mice, and loss-of-function mutations in MC4R in humans, are associated with severe obesity and hyperinsulinemia, supporting an essential role for the melanocortin system

in the regulation of glucose metabolism [36, 37]. It was shown that the renal sympathoexcitatory responses to leptin and insulin are dependent on the MC4R, suggesting an important role for the MC4R in the regulation of renal sympathetic nerve outflow [38]. In addition, MC4R is found in numerous brain nuclei [33, 37, 39-42], including the sites known to be in the autonomic circuitry of the kidney, such as the hypothalamic paraventricular nucleus (PVH), the dorsomedial hypothalamus (DMH), the raphe pallidus (RPa) of the brainstem, etc [43-45]. However, the exact neurosubstrate underlying the regulation of renal function by the central melanocortin system has not been well defined. The main objective of this study is to provide direct neuroanatomical evidence for the central melanocortin circuits connecting to renal tissues via autonomic nervous system.

RESULTS

Time course of multisynaptic CNS projections to the kidney

The entire spinal cord and brain were examined for PRV-614 and MC4R-GFP immunoreactivity. Viral immunoreactive labeling was monitored at 1-day intervals, up to 6 days after renal injection. Postinjection intervals shorter than 3 days (1~2 day) did not result in viral labeling of any neurons in the CNS.

After 3 days of renal PRV-614 infection ($n = 3$, phase I), colocalization of PRV-614 and MC4R-GFP immunopositive neurons was seen and largely confined to
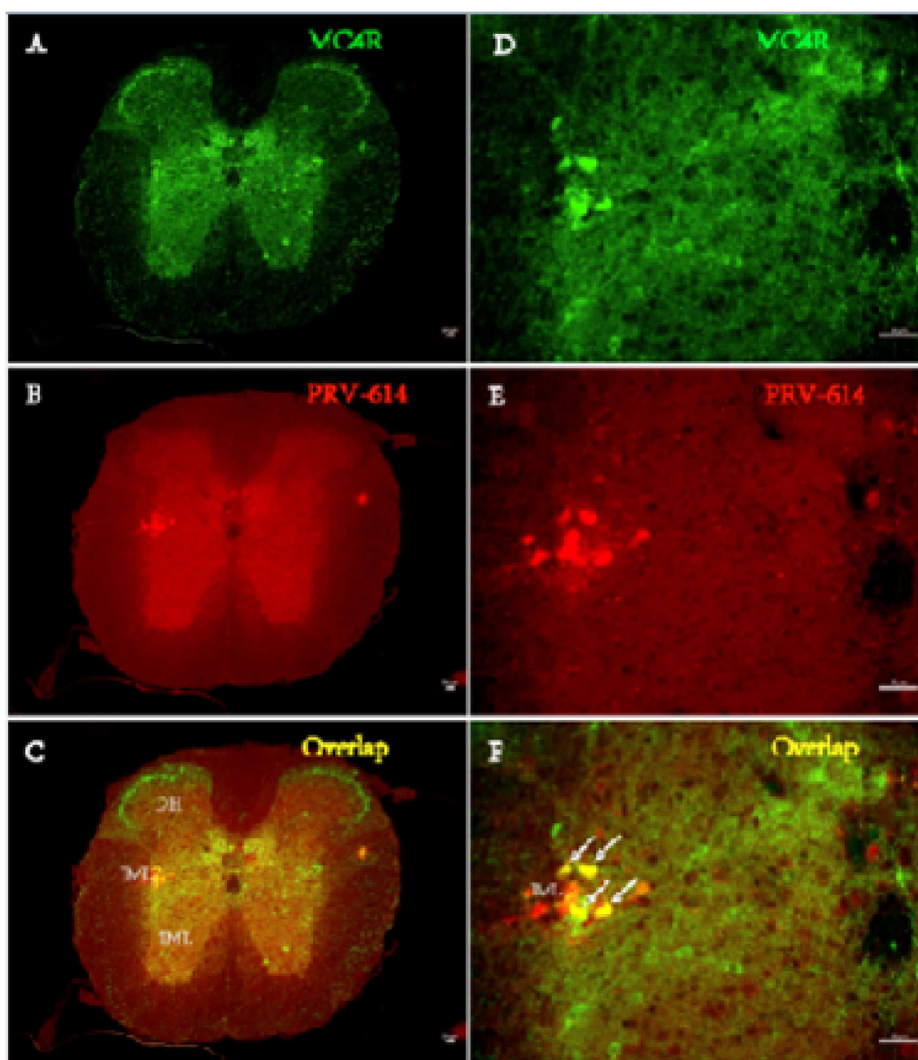

Figure 1: Fluorphor expression illustrating the distributions of PRV-614 (red) and MC4R (green) in transverse section of spinal cord IML in MC4R-GFP transgenic mice. Infected sympathetic preganglionic neurons (SPN) neurons in the thoracic IML 4 days after injection of PRV-614 into the kidneys are illustrated. **A.** MC4R-GFP expressing neurons; **B.** PRV-614 expressing neurons in same section as (A); **C.** overlap of (A) and (B), depicting distribution of MC4R-GFP-IR and PRV-614-bearing neurons (while arrow). **D.**, **E.** and **F.**, amplified views of (A, B and C), respectively. IML, the intermediolateral cell column; IC intercalates nucleus; CAN, central autonomic nucleus; DH, Dorsal horn; VH, ventral horn. Scale bar: 50μm.

areas in the sympathetic preganglionic neurons (SPNs) in the ipsilateral intermediolateral cell column (IML) of the thoracic spinal cord (Figure 1). Additionally, the kidneys of two mice began to show colocalization of PRV-614 and MC4R-GFP in the paraventricular nucleus of the hypothalamus (PVN).

At 4 days after kidney injection ($n = 3$, phase II), PRV-614 immunopositive neurons were detected in the brainstem (e.g., rostral ventrolateral medulla (RVLM), A5 noradrenergic cell region (A5) and nucleus of the solitary tract (NTS), Figure 2) and the paraventricular nucleus of the hypothalamus (PVN) that give rise to direct descending projections to IML of the thoracic spinal cord. The majority of MC4R-GFP/PRV-614 double-labeled neurons were found in the PVN, raphe nuclei (RPa) and NTS, and with a less extent in the RVLM and A5.

At 5 days postinjection ($n = 4$, phase III), the number of PRV-614 infected neurons in regions shown at 4 days was increased and the infection spread transneuronally to neurons in other regions of the medulla (e.g., nuclei raphes,
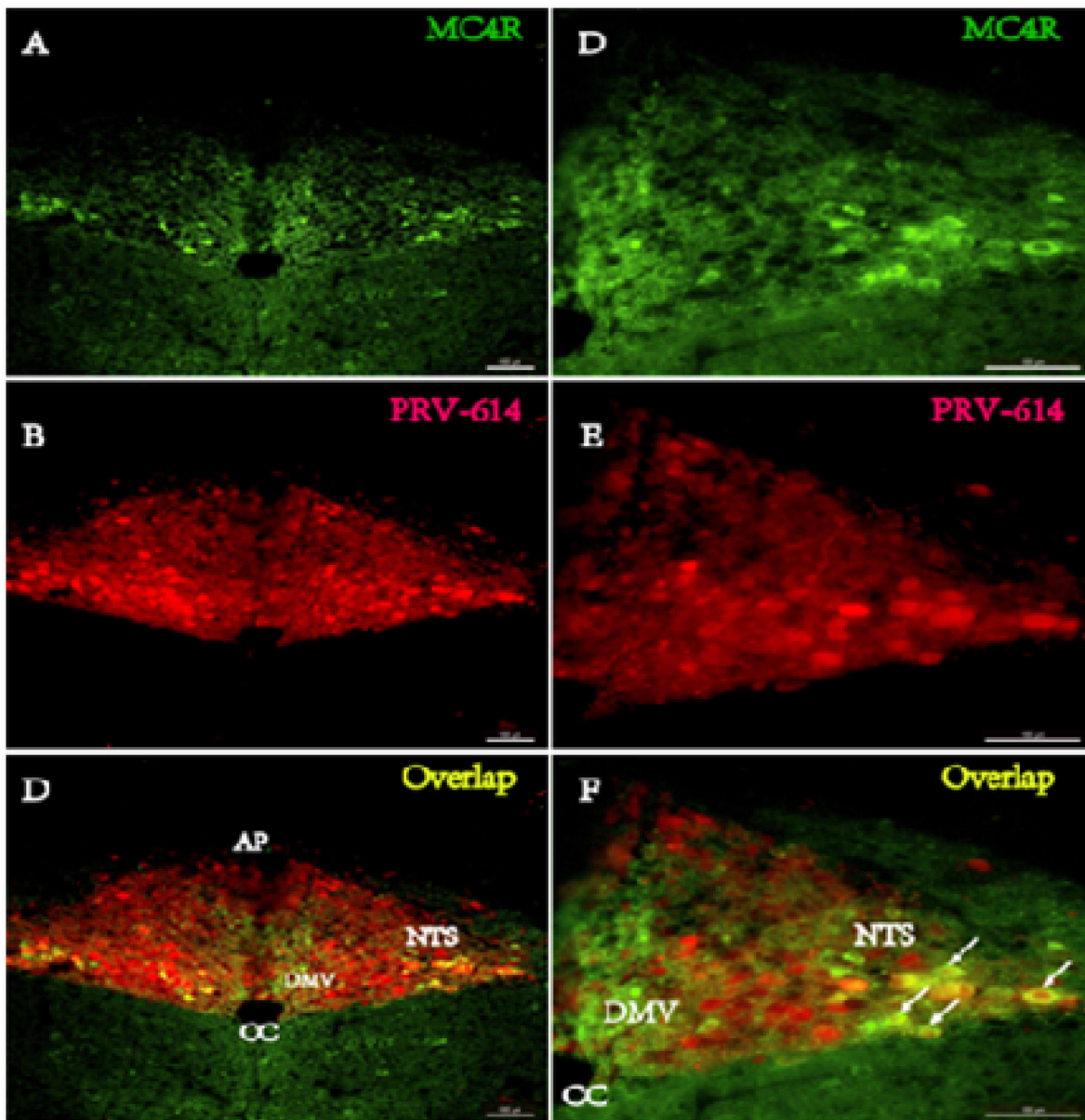

Figure 2: Fluorphor expression illustrating the distributions of PRV-614 (red) and MC4R (green) in the caudal brainstem in MC4R-GFP transgenic mice. A.-C. Low magnification images of a section from the caudal brainstem obtained 4 d after the kidney was injected with PRV-614-ERFP (A, red) and labeled with MC4R-GFP (B, green). C). The images in A and B have been merged with an image showing NTS neurons retrogradely labeled by intra-kidney injection of PRV-614-ERFP. Note that viral labeling is absent in the DMV and restricted to a subset of neurons in the known location of NTS. **D.-E.** High magnification images of the region in panel C, to show the overlap of the viral label (D) and the MC4R-GFP (E) in NTS neurons. F). Merged image of D and E. Scale bars: 50 μm. AP, area postrema; CC, Central canal; DMV, dorsal motor nucleus of the vagus; NTS, Nucleus of the solitary tract.

Figure 3, 4, rostral ventromedial medulla (RVMM), Figure 3,4, locus coeruleus (LC)), midbrain (e.g., periaquaductal gray (PAG)) and hypothalamus. Of particular note, colocalization of PRV-614 and MC4R-GFP began to become more widespread. Colocalization was still apparent in the RPa, NTS and PVN as well as in several new regions. Double-labeled neurons were concentrated in the rostral ventromedial medulla (e.g., raphe nuclei, NRM, and NGCα) , Figure 3, 4, the dorsal brainstem (e.g., NTS), the dorsolateral pons (e.g., Barrington's nucleus and SubC), midbrain (e.g., PAG), and hypothalamus (e.g., PVN, LH). In the PVN (Figure 5), coexpression in all the animals was observed at d5, as well as a large increase in the number of PRV-614-infected neurons, primarily in the ventromedial parvocellular PVN and lateral parvicellular PVN (coexpression in 8% of all PRV-614-infected neurons and 30% of all MC4R neurons in the PVN). The number of singly labeled PRV-614 neurons and the number of colocalized neurons at d5 were increased than that at d4 in the RVMM (coexpression in 12% of all PRV-614-infected neurons and 35% of all MC4R-expressing neurons at d5),

in the RPa (coexpression in 12% of all PRV-614-infected neurons and 30% of all MC4R-expressing neurons at d5) and the NTS (coexpression in 10% of all PRV-614-infected neurons and 16% of all MC4R-expressing neurons at d5). The first colocalized neurons were detected in the lateral hypothalamus at d5, and in spite of being small in number, they were observed in all animals (coexpression in 12% of all PRV-614-infected neurons and 20% of all MC4R-expressing neurons at d5).

Areas with PRV-614 staining during phase IV ($n = 6$, 6-7 days postinjection) revealed PRV-614 expression in the majority of hypothalamic sites such as the ventromedial hypothalamus (VMH), lateral hypothalamus (LH), arcuate nucleus (ARC), and preoptic area (POA) as well as motor cortex (M1-M2). Colocalization of PRV-614 and MC4R-GFP was seen in all the same regions as at d5 with small increases in the number of PRV-614-infected neurons in those areas. New regions containing double-labeled PRV-614/MC4R-GFP neurons include the hypothalamus [PVN, DMH, VMH, Arc, retrochiasmatic area (RCh), POA], and forebrain [e.g., motor cortex, Amygdala, central nucleus
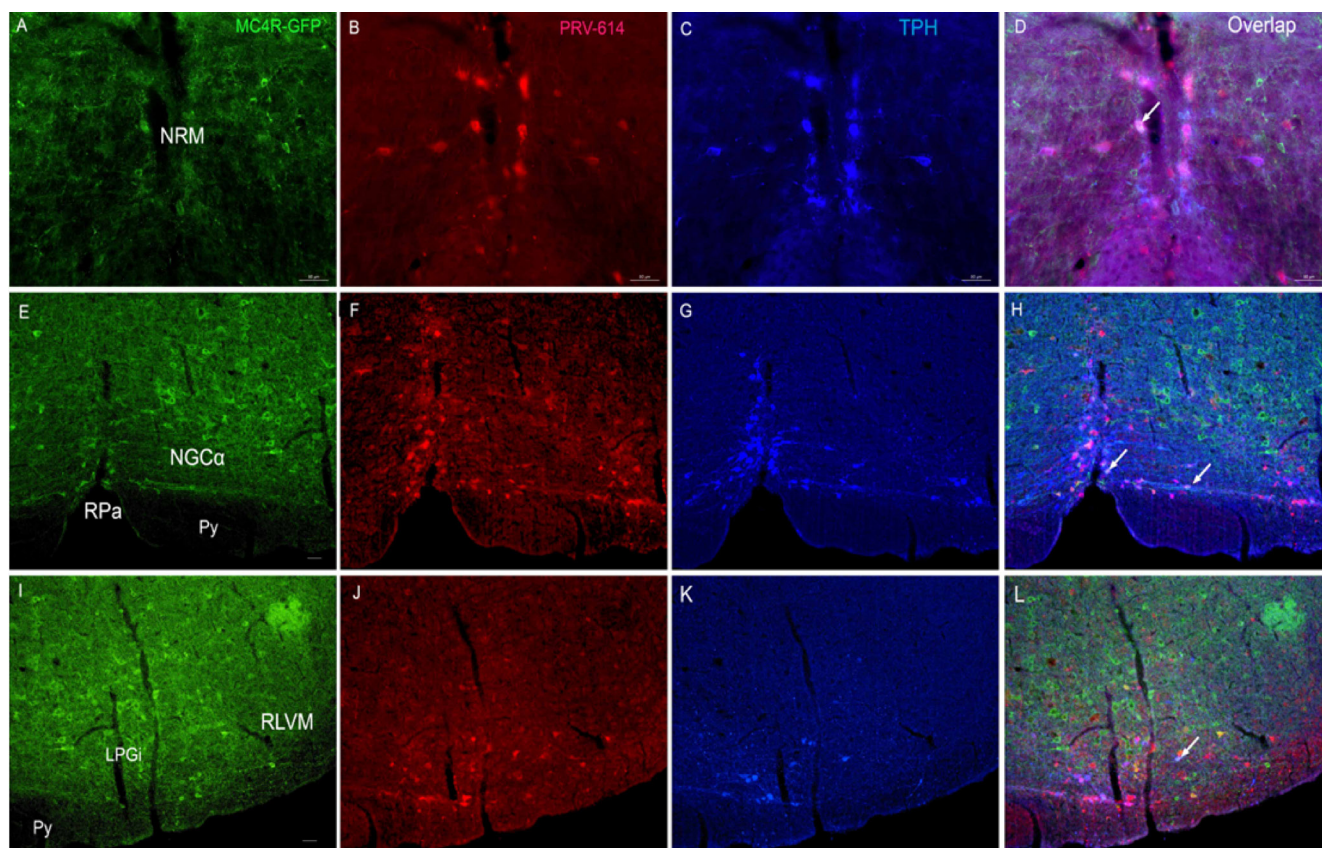

Figure 3: Triple fluorphor expression in the ventral brainstem 5 days after renal PRV-614 injection of MC4R-GFP transgenic mice. D. Distributions of MC4R-GFP- (**A.**, green), PRV-614 (**B.**, red) and TPH-IR-cells (**C.**, blue) in the NRM 5 days after renal PRV-614 injection; **H.** Distributions of MC4R-GFP- (**E.**, green), PRV-614 (**F.**, red) and TPH-IR-cells (**G.**, blue) in the RPa and NGCα 5 days after renal PRV-614 injection; L) Distributions of MC4R-GFP-(**I.**, green), PRV-614-(**J.**, red) and TPH-IR-cells (**K.**, blue) in the LPGi 5 days after renal PRV-614 injection. Triple-labeled cells were indicated by white arrows. Scale bar: A-D for 50 μm; E-H for 25 μm; I-L for 50 μm. LPGi, lateral gigantocellular reticular nucleus; NGCα, gigantocellular reticular nucleus α part; NRM, nucleus raphe magnus; Py, pyramidal tract; RLVM, lateral ventromedial medulla; RPa, the raphe pallidus.

of amygdale (CeM), bed nucleus of the stria terminalis (BST)]. From d5 to d6-7, the most substantial increase seen in the number of PRV-infected and colocalized cells was in the PVN (coexpression in 23.8% of all PRV-infected neurons and 38.5% of all MC4R-expressing neurons in d 6). The first colocalized neurons were detected in the motor cortex at d6, they were observed in all animals (coexpression in 41.5% of all PRV-infected neurons and 22.7% of all MC4R-expressing neurons).

Infection of serotonergic neurons following injections of PRV-614 into the kidney

Because a portion of neurons that participate in regulating sympathetic outflow expresses serotonin [46-50], we ascertained whether MC4R-GFP-positive neurons infected after the injection of PRV-614 into the left kidney were serotonergic (5-HT and TPH immunoreactivity positive neurons). Previous studies suggested that TPH-expressing neurons were observed within distinct subdivisions of the CNS, including raphe, VMM, lateral paragigantocellular cell group (LPGi), dorsal raphe (DR), and PVN [51]. In this study, the analysis was limited to the five brain areas containing an appreciable number of PRV-614-infected cells: raphe, VMM, LPGi, DR and PVN. PRV-614/TPH dual-labeled cells and MC4R/PRV-614/TPH triple-labeled cells were present in raphe, VMM, LPGi, and PVN, and the number of dual-labeled cells was much higher than that of triple-labeled cells (Figure 4 and 5). No triple-labeled cells were observed in DR.

DISCUSSION

To date, this is the first study to explore the neurochemical phenotype of the neurons belonging to the central melanocortinergic efferent pathways innervating the kidneys. PRV-614 retrogradely labeled neurons were found in numerous CNS regions [43, 45, 50, 52], but the proportion of these neurons possessing MC4R-GFP were mainly located in IML of the thoracic spinal cord, the PVN of the hypothalamus, and RPa, NRM and VMM
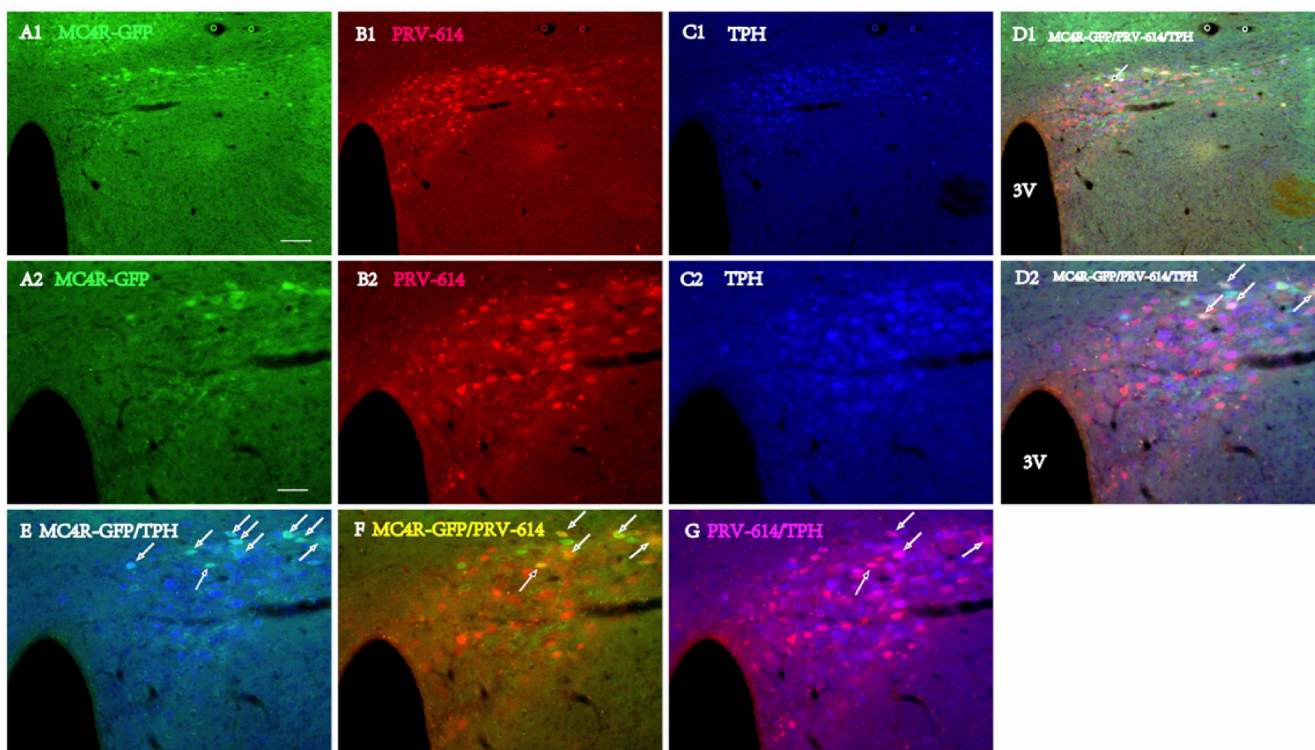

Figure 4: Triple fluorophor Expression in Diencephalon and the paraventricular hypothalamic nucleus (PVN) 6 days after renal PRV-614 injection of MC4R-GFP transgenic mice. A1. MC4R-GFP neurons (green) in the PVN, **B1.,** same section as (A1), and the distribution of PRV-614 infected neurons in diencephalon at the level of the PVN is illustrated. **D1.** Distributions of MC4R-GFP- (A1, green), PRV-614 (B1, red) and TPH-IR-cells (**C1.**, blue) in the PVN 6 days after renal PRV-614 injection; **A2.** A higher magnification image of (A1) showing MC4R-bearing neurons in the RPa (green), **B2.** Same section as **A2.**, depicting PRV-614-infected neurons (red), **C2.** Same section as **A2.**, depicting TPH positive neurons (blue), **D2.,** Same section as (A2), and triple-labeled cells were indicated by white arrows. **E.** Overlap of (A2) and (C2), depicting the neurons that co-express PRV-614 and TPH (cyan, with white arrows). **F.** Overlap of (A2) and (B2), depicting the neurons that co-express PRV-614 and MC4R-GFP (yellow, with white arrows). **G.** Overlap of (B2) and (C2), depicting the neurons that co-express PRV-614 and TPH (pink, with white arrows). Scale bar: A1-D1 for 50 μm; A2-D2, E-G for 100 μm.

of the brainstem which were believed to be related to the control of energy homeostasis [53].

In this study, we focused principally on those PRV-614-infected areas (neurons) that also express MC4R. Transsynaptic tracing by injection of attenuated PRV-614 into the kidneys in MC4R-GFP transgenic mice, coupled with dual or triple-labeling immunohistochemical techniques, reveals a specific subset of dual or triple-labeled MC4R-GFP/PRV-IR neurons in multiple nuclei at various levels of the CNS. The majority of MC4R-GFP/PRV-614 double-labeled neurons were found in the RPa, NRM and VMM, and with a less extent in the RVLM, A5, and LC. Most of the double-labeled PRV-614/TPH neurons were located in the RPa, NRM and VMM. Accordingly, it seems logical that most of the triple-labeled MC4R-GFP/PRV-614/TPH neurons were located in the same brain regions, i.e., RPa, NRM and VMM. The data presented support previous tracing and neurophysiological investigations that the MC4R signaling pathway, constituting a major signaling system in the control of energy homeostasis [15], is functionally distributed both in the hypothalamus and the brainstem [53], suggesting a broad central melanocortinergic neurons involved in kidney control. The PVN is now commonly recognized as an important brain region exerting prominent influences over endocrine and autonomic regulation [52]. A large number of significant scientific reports demonstrated MC4R in the PVN is important in regulating energy balance and sympathetic activity [54]. The existence of double- and triple-labeled neurons in the PVN is consistent with the proposed role of this brain region.

A considerable amount of literature had demonstrated that serotonin and leptin shared a similar signaling mechanism regulating energy balance and glucose homeostasis *via* actions within the CNS [55]. In the absence of leptin receptors, the renal sympathoexcitatory effects of melanocortin system
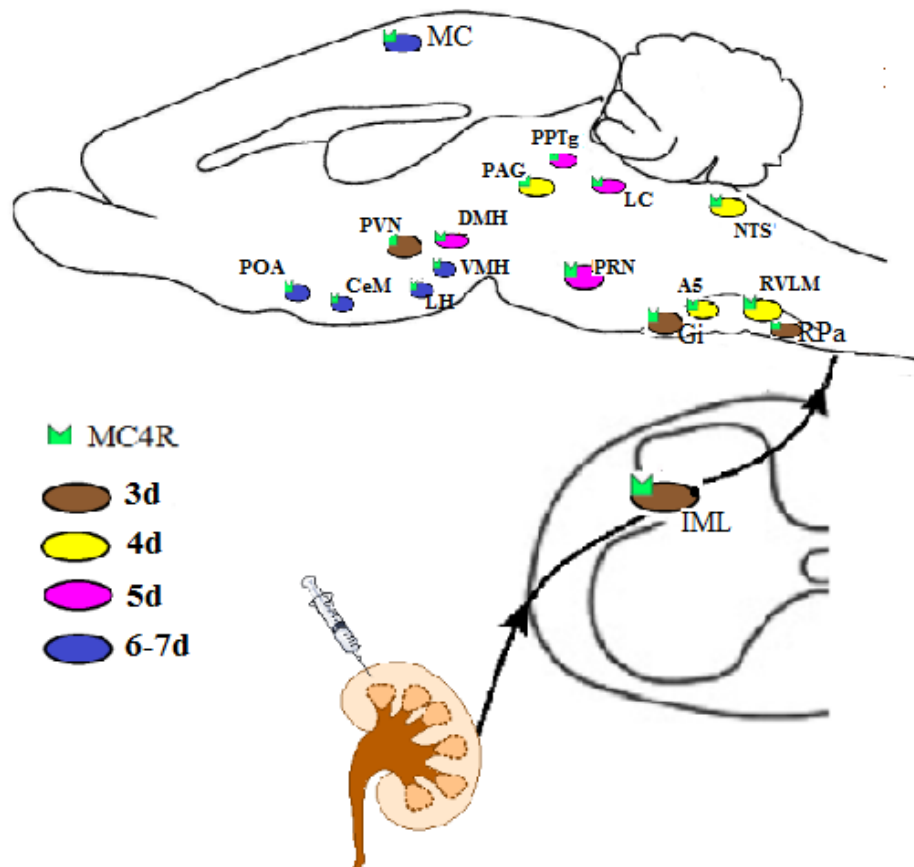

Figure 5: Schematic diagram showing MC4R-expressing areas in the mouse brain infected at different intervals after PRV-614 injection into kidney (brown, 3d; yellow, 4d; purple, 5d; blue, 6-7d), suggesting that MC4R signaling in the neural circuitry controlling the kidneys mediated by sympathetic pathway. A5, A5 noradrenergic cell region; CeM, central nucleus of the amygdala; DMH, dorsomedial nucleus of the hypothalamus; Gi, gigantocellular reticular nucleus; IML, intermediolateral cell column;LC, Locus ceruleus; LH, lateral hypothalamus; LPB, lateral parabrachial nucleus; LTD, laterodorsal tegmental nucleus; MC, motor cortex; MC4R, melanocortin4receptor; NTS, nucleus of the solitary tract; PAG, periaqueductal gray; PRN, pontine reticular nucleus; POA, preoptic area; PPTg, pedunculopontine tegmental nucleus; PVN, paraventricular nucleus of the hypothalamus; RPa, raphe pallidus; VMH, ventromedial hypothalamic nucleus.

stimulation were attenuated [38]. 5-HT2CR agonists improved glucose homeostasis *via* increased production and release of endogenous melanocortin agonists, with subsequent activation of sympathetic preganglionic neurons in the IML *via* stimulation of MC4R [56] . These data suggested the major rodent brain regions that contain MC4R and TPH, involved in the descending pathways that control the kidneys.

In conclusion, the present results reveal a hierarchical organization of the descending MC4R neuronal circuits controlling the kidney, thus providing the neuroanatomical support for the role of the MC4R, and to a less extent TPH, in the control of kidneys.

MATERIALS AND METHODS

Animal care

The transgenic mice carrying green fluorescent protein (GFP) under the control of the melanocortin-4 receptor promoter coupled with the cytomegalovirus (CMV) immediate early enhancer, were first obtained from Dr. Joel Elmquist (UT Southwestern Medical Center) and then bred to generate male and female mice. Genotyping was performed by PCR as described in previous studied [17, 57]. All mice used were weighted between 25-30 g and maintained in a standard 12h light-dark cycle with *ad libitum* access to food and water in a temperature-controlled room. All studies involving the animals were performed following the National Guides for the Care and Use of Laboratory Animals and approved by the Institutional Animal Care and Use Committee of Tongji Hospital, Tongji Medical College, Huazhong University of Science and Technology University, Wuhan, China.

Surgical procedures, PRV-614 injection and post-surgical care

To provide a description of the pattern and temporal progression of viral infection resulting from injection of PRV-614 into the kidney, virus was injected into the left kidneys of mice. PRV-614 is a specific trans-synaptic retrograde tracer from axon terminals to the cell nucleus, where replication occurs [2, 27, 58]. Under full anesthesia with isoflurane, the skin overlying the kidney was incised by ventral midline laparotomy to expose the upper pole of the kidney [59, 60]. Sixteen mice received a series of injections with PRV-614 (2×10^8 pfu/ml in a total of 1 μl per injection at five injection sites per kidney) into the upper pole of the visualized left kidney using a 30-gauge needle connected to a Hamilton syringe (10 μl) under microscopic guidance. After the final injection, the renal surface was rinsed twice with sterile saline-soaked swabs and blotted dry. The kidney was then returned to the abdominal cavity. The abdominal muscle incision was closed with silk sutures, and the skin incision was closed with stainless steel wound clips. The time course of infection was empirically determined by observing the pattern of infection at exactly 3- ($n = 3$), 4- ($n = 3$), 5- ($n = 4$), 6-day ($n = 3$) and 7-day ($n = 3$) survival time. The mice were provided with analgesia with an intramuscular injection of a mixture of ketamine (10 mg/kg) and ketoprofen (3 mg/kg) just before the surgery and every 12 hours subsequently during a post-surgical period of 72 hours. Mice infected with PRV-614 remained asymptomatic until 5-6 days after virus injection, and they were euthanized either before or when they showed apparent traits of illness or distress (i.e. 6-7 days after inoculation).

Perfusion and fluorescence immunohistochemistry

After a survival time of 3-6 days, mice were deeply anesthetized with an overdose of urethane and perfused with 0.9% saline, which was followed by 4% paraformaldehyde-borate fixative (pH 9.5) *via* the left ventricle. Spinal cord and brain were removed and post-fixed in 4% paraformaldehyde-borate overnight at room temperature and in a 30% sucrose solution for 2 days at 4°C. Post-fixed spinal cord and brains were blocked, and sliced at 30 μm/coronal section on a freezing-stage sledge microtome, and collected into four serially ordered sets of sections through its rostrocaudal extent. Tissue sections were stored at 4°C until they were processed for immunohistochemical visualization.

To determine which PRV-614-immunoreactive (IR) neurons coexpressing MC4R-GFP, distinct fluorophores were used for PRV-614 and GFP. The fluorescence immunohistochemical (IHC) procedure was carried out according to published protocols [40, 61]. In brief, the tissue sections were incubated at 4°C overnight in 0.02M potassium PBS (KPBS; pH7.4), and washed with 0.01M phosphate buffered saline (PBS) (3×10min). Sections were pre-treated for 25 min in 1% sodium borohydride in 0.01M PBS, and washed in 0.01M PBS (3×10min). Sections were blocked for 60min in 0.02M KPBS containing 2% normal donkey serum (Jackson ImmunoResearch, West Grove, PA) and 0.4% Triton X-100 (Sigma, St. Louis, MO), and treated further by washing with 0.01M PBS (3×10min). Sections were incubated with guinea-pig polyclonal antibody against PRV (1:5000; National Institute of Allergy and Infectious Diseases, Bethesda, MD) and a rabbit polyclonal antibody against GFP (1:10,000; Molecular Probes, Eugene, OR) in 0.02M KPBS containing 0.4% Triton X-100 for 48 h at 4°C, with gentle agitation. Sections were then rinsed several times in 0.01M PBS over a 1-h period followed by incubation with Cy3-conjugated donkey anti-guinea pig IgG (1:2000; Jackson ImmunoResearch Laboratories Inc, West Grove, PA) and Alexafluor 488-conjugated donkey anti-rabbit IgG

(H+L) (1:1000; Molecular Probes, Eugene, OR) in KPBS containing 0.4% Triton-X-100 for 1h at room temperature. Sections were then rinsed thoroughly in 0.01M PBS. All sections were mounted onto slides, air dried, and cover slipped with mounting media.

Brain sections were also processed for the triple localization of PRV-614, MC4R-GFP, and TPH. The processing of this tissue was similar to that described above. For TPH IHC, first antibody used for immunohistochemical analysis was sheep anti-TPH (1:2000; Chemicon International, Temecula, CA) and second antibody included biotinylated Donkey anti-sheep Ig (H+L) (Lot no.68003, Jackson ImmunoResearch Lab., West Grove, PA) and streptavidin Alexa Fluor 350 conjugate (Lot no.49248A, S-11249, Invitrogen, Molecular Probes, Eugene, OR). After the completion of immunohistochemical processing, the sections were mounted on gelatin-coated slides, dehydrated, cleared, and cover slipped with the use of mounting media. In negative control incubations, the primary antiserums were omitted from the immunohistochemical reaction. This procedure completely eliminated neuronal staining.

Tissue analysis

The regions in which infected cells were located were defined with reference to the atlases of Franklin KB and Paxinos G [62] and a study by Molander and colleagues [63] that were used to guide the spinal cord tissue analysis. Immunofluorescence photomicroscope was achieved by using the Leica Microsystems (DM400B, Wetzlar, Germany) with a filter set for visualization of Alexafluor 488 (excitation range, 425-525 nm; emission range, 500-600 nm), Cy3 (excitation range, 500-560 nm; emission range, 560-650 nm) and Alexafluor 350 (excitation range, 300-400 nm; emission range, 440-490 nm). PRV-614 infected neurons are identified with red fluorescence, MC4R-expressing neurons by green fluorescence, and TPH-expressing neurons by blue fluorescence. Images were overlaid using Adobe Photoshop, and double-labeled neurons are presented as yellow (red/green) or pink (red/blue). High-magnification analysis was used to determine whether overlapping yellow or pink images were due to colocalization in the same neuron or overlap of independently labeled neurons.

CONFLICTS OF INTEREST

The authors have no conflict of interest related to this paper.

REFERENCES

1. Huang J, Chowhdury SI and Weiss ML. Distribution of sympathetic preganglionic neurons innervating the kidney in the rat: PRV transneuronal tracing and serial reconstruction. Auton Neurosci. 2002; 95:57-70.

2. Hao Y, Tian XB, Liu C and Xiang HB. Retrograde tracing of medial vestibular nuclei connections to the kidney in mice. International journal of clinical and experimental pathology. 2014; 7:5348-5354.

3. Liu C, Ye DW, Guan XH, Li RC, Xiang HB and Zhu WZ. Stimulation of the pedunculopontine tegmental nucleus may affect renal function by melanocortinergic signaling. Med Hypotheses. 2013; 81:114-116.

4. Coote JH. A role for the paraventricular nucleus of the hypothalamus in the autonomic control of heart and kidney. Exp Physiol. 2005; 90:169-173.

5. Badoer E. Role of the hypothalamic PVN in the regulation of renal sympathetic nerve activity and blood flow during hyperthermia and in heart failure. Am J Physiol Renal Physiol. 2010; 298:F839-846.

6. Chen AD, Zhang SJ, Yuan N, Xu Y, De W, Gao XY and Zhu GQ. Angiotensin AT1 receptors in paraventricular nucleus contribute to sympathetic activation and enhanced cardiac sympathetic afferent reflex in renovascular hypertensive rats. Exp Physiol. 2011; 96:94-103.

7. Freeman KL and Brooks VL. AT(1) and glutamatergic receptors in paraventricular nucleus support blood pressure during water deprivation. Am J Physiol Regul Integr Comp Physiol. 2007; 292:R1675-1682.

8. Gerich JE, Meyer C, Woerle HJ and Stumvoll M. Renal gluconeogenesis: its importance in human glucose homeostasis. Diabetes Care. 2001; 24:382-391.

9. Marsenic O. Glucose control by the kidney: an emerging target in diabetes. Am J Kidney Dis. 2009; 53:875-883.

10. Sabharwal R, Coote JH, Johns EJ and Egginton S. Effect of hypothermia on baroreflex control of heart rate and renal sympathetic nerve activity in anaesthetized rats. J Physiol. 2004; 557:247-259.

11. Pyner S, Deering J and Coote JH. Right atrial stretch induces renal nerve inhibition and c-fos expression in parvocellular neurones of the paraventricular nucleus in rats. Exp Physiol. 2002; 87:25-32.

12. Dibona GF. Differentiation of vasoactive renal sympathetic nerve fibres. Acta Physiol Scand. 2000; 168:195-200.

13. DiBona GF. Neural control of the kidney: functionally specific renal sympathetic nerve fibers. Am J Physiol Regul Integr Comp Physiol. 2000; 279:R1517-1524.

14. Ye DW, Liu C, Liu TT, Tian XB and Xiang HB. Motor cortex-periaqueductal gray-spinal cord neuronal circuitry may involve in modulation of nociception: a virally mediated transsynaptic tracing study in spinally transected transgenic mouse model. PLoS One. 2014; 9:e89486.

15. Greenfield JR, Miller JW, Keogh JM, Henning E, Satterwhite JH, Cameron GS, Astruc B, Mayer JP, Brage S, See TC, Lomas DJ, O'Rahilly S and Farooqi IS. Modulation of blood pressure by central melanocortinergic pathways. N Engl J Med. 2009; 360:44-52.

16. Heisler LK, Cowley MA, Kishi T, Tecott LH, Fan W, Low MJ, Smart JL, Rubinstein M, Tatro JB, Zigman JM, Cone RD and Elmquist JK. Central serotonin and melanocortin pathways regulating energy homeostasis. Annals of the New York Academy of Sciences. 2003; 994:169-174.

17. Rossi J, Balthasar N, Olson D, Scott M, Berglund E, Lee CE, Choi MJ, Lauzon D, Lowell BB and Elmquist JK. Melanocortin-4 receptors expressed by cholinergic neurons regulate energy balance and glucose homeostasis. Cell Metab. 2011; 13:195-204.

18. Mirshahi UL, Still CD, Masker KK, Gerhard GS, Carey DJ and Mirshahi T. The MC4R(I251L) allele is associated with better metabolic status and more weight loss after gastric bypass surgery. J Clin Endocrinol Metab. 2011; 96:E2088-2096.

19. Siljee-Wong JE. Melanocortin MC(4) receptor expression sites and local function. Eur J Pharmacol. 2011; 660:234-240.

20. Hatoum IJ, Stylopoulos N, Vanhoose AM, Boyd KL, Yin DP, Ellacott KL, Ma LL, Blaszczyk K, Keogh JM, Cone RD, Farooqi IS and Kaplan LM. Melanocortin-4 receptor signaling is required for weight loss after gastric bypass surgery. J Clin Endocrinol Metab. 2012; 97:E1023-1031.

21. Xu LJ, Liu TT, He ZG, Hong QX and Xiang HB. Hypothesis: CeM-RVLM circuits may be implicated in sudden unexpected death in epilepsy by melanocortinergic-sympathetic signaling. Epilepsy & behavior. 2015; 45:124-127.

22. Xu AJ, Liu TT, He ZG, Wu W and Xiang HB. CeA-NPO circuits and REM sleep dysfunction in drug-refractory epilepsy. Epilepsy & behavior. 2015; 51:273-276.

23. Xu AJ, Liu TT, He ZG, Hong QX and Xiang HB. STN-PPTg circuits and REM sleep dysfunction in drug-refractory epilepsy. Epilepsy & behavior. 2015; 51:277-280.

24. He ZG, Liu BW and Xiang HB. Cross interaction of melanocortinergic and dopaminergic systems in neural modulation. International journal of physiology, pathophysiology and pharmacology. 2015; 7:152-157.

25. Hao Y, Tian XB, Liu TT, Liu C, Xiang HB and Zhang JG. MC4R expression in pedunculopontine nucleus involved in the modulation of midbrain dopamine system. International

journal of clinical and experimental pathology. 2015; 8:2039-2043.

26. Hao Y, Liu TT, He ZG, Wu W and Xiang HB. Hypothesis: CeM-PAG GABAergic circuits may be implicated in sudden unexpected death in epilepsy by melanocortinergic signaling. Epilepsy & behavior. 2015; 50:25-28.

27. Xiang HB, Liu C, Liu TT and Xiong J. Central circuits regulating the sympathetic outflow to lumbar muscles in spinally transected mice by retrograde transsynaptic transport. International journal of clinical and experimental pathology. 2014; 7:2987-2997.

28. Ke B, Liu TT, Liu C, Xiang HB and Xiong J. Dorsal subthalamic nucleus electrical stimulation for drug/treatment-refractory epilepsy may modulate melanocortinergic signaling in astrocytes. Epilepsy & behavior. 2014; 36:6-8.

29. Hong Q, Fang G, Liu TT, Guan XH, Xiang HB and Liu Z. Posterior pedunculopontine tegmental nucleus may be involved in visual complaints with intractable epilepsy. Epilepsy & behavior. 2014; 34C:55-57.

30. Hao Y, Guan XH, Liu TT, He ZG and Xiang HB. Hypothesis: The central medial amygdala may be implicated in sudden unexpected death in epilepsy by melanocortinergic-sympathetic signaling. Epilepsy & behavior. 2014; 41C:30-32.

31. Feng L, Liu TT, Ye DW, Qiu Q, Xiang HB and Cheung CW. Stimulation of the dorsal portion of subthalamic nucleus may be a viable therapeutic approach in pharmacoresistant epilepsy: A virally mediated transsynaptic tracing study in transgenic mouse model. Epilepsy & behavior. 2014; 31C:114-116.

32. Fan W, Dinulescu DM, Butler AA, Zhou J, Marks DL and Cone RD. The central melanocortin system can directly regulate serum insulin levels. Endocrinology. 2000; 141:3072-3079.

33. Liu H, Kishi T, Roseberry AG, Cai X, Lee CE, Montez JM, Friedman JM and Elmquist JK. Transgenic mice expressing green fluorescent protein under the control of the melanocortin-4 receptor promoter. J Neurosci. 2003; 23:7143-7154.

34. Sayk F, Heutling D, Dodt C, Iwen KA, Wellhoner JP, Scherag S, Hinney A, Hebebrand J and Lehnert H. Sympathetic function in human carriers of melanocortin-4 receptor gene mutations. J Clin Endocrinol Metab. 2010; 95:1998-2002.

35. Matsumura K, Tsuchihashi T, Abe I and Iida M. Central alpha-melanocyte-stimulating hormone acts at melanocortin-4 receptor to activate sympathetic nervous system in conscious rabbits. Brain Res. 2002; 948:145-148.

36. Huszar D, Lynch CA, Fairchild-Huntress V, Dunmore JH, Fang Q, Berkemeier LR, Gu W, Kesterson RA, Boston BA, Cone RD, Smith FJ, Campfield LA, Burn P, et al. Targeted disruption of the melanocortin-4 receptor results in obesity in mice. Cell. 1997; 88:131-141.

37. Cone RD. Anatomy and regulation of the central melanocortin system. Nat Neurosci. 2005; 8:571-578.

38. Rahmouni K, Haynes WG, Morgan DA and Mark AL. Role of melanocortin-4 receptors in mediating renal sympathoactivation to leptin and insulin. J Neurosci. 2003; 23:5998-6004.

39. Mountjoy KG, Mortrud MT, Low MJ, Simerly RB and Cone RD. Localization of the melanocortin-4 receptor (MC4-R) in neuroendocrine and autonomic control circuits in the brain. Mol Endocrinol. 1994; 8:1298-1308.

40. Voss-Andreae A, Murphy JG, Ellacott KL, Stuart RC, Nillni EA, Cone RD and Fan W. Role of the central melanocortin circuitry in adaptive thermogenesis of brown adipose tissue. Endocrinology. 2007; 148:1550-1560.

41. Liu TT, He ZG, Tian XB, Liu C, Xiang HB and Zhang JG. Hypothesis: Astrocytes in the central medial amygdala may be implicated in sudden unexpected death in epilepsy by melanocortinergic signaling. Epilepsy & behavior. 2015; 42:41-43.

42. Liu TT, He ZG, Tian XB and Xiang HB. Neural mechanisms and potential treatment of epilepsy and its complications. Am J Transl Res. 2014; 6:625-630.

43. Cano G, Card JP and Sved AF. Dual viral transneuronal tracing of central autonomic circuits involved in the innervation of the two kidneys in rat. J Comp Neurol. 2004; 471:462-481.

44. Xiang HB, Liu C, Guo QQ, Li RC and Ye DW. Deep brain stimulation of the pedunculopontine tegmental nucleus may influence renal function. Med Hypotheses. 2011; 77:1135-1138.

45. Zermann DH, Ishigooka M, Doggweiler-Wiygul R, Schubert J and Schmidt RA. Central autonomic innervation of the kidney. What can we learn from a transneuronal tracing study in an animal model? The Journal of urology. 2005; 173:1033-1038.

46. Pan XC, Song YT, Liu C, Xiang HB and Lu CJ. Melanocortin-4 receptor expression in the rostral ventromedial medulla involved in modulation of nociception in transgenic mice. Journal of Huazhong University of Science and Technology Medical sciences. 2013; 33:195-198.

47. Wei F, Dubner R, Zou S, Ren K, Bai G, Wei D and Guo W. Molecular depletion of descending serotonin unmasks its novel facilitatory role in the development of persistent pain. J Neurosci. 2010; 30:8624-8636.

48. Nakamura K and Morrison SF. Central efferent pathways mediating skin cooling-evoked sympathetic thermogenesis in brown adipose tissue. Am J Physiol Regul Integr Comp Physiol. 2007; 292:R127-136.

49. Nakamura K, Matsumura K, Kaneko T, Kobayashi S, Katoh H and Negishi M. The rostral raphe pallidus nucleus mediates pyrogenic transmission from the preoptic area. J Neurosci. 2002; 22:4600-4610.

50. Card JP, Kobiler O, McCambridge J, Ebdlahad S, Shan Z, Raizada MK, Sved AF and Enquist LW. Microdissection of neural networks by conditional reporter expression from a Brainbow herpesvirus. Proc Natl Acad Sci U S A. 2011; 108:3377-3382.

51. Manger PR, Fahringer HM, Pettigrew JD and Siegel JM. The distribution and morphological characteristics of serotonergic cells in the brain of monotremes. Brain Behav Evol. 2002; 60:315-332.

52. Card JP, Kobiler O, Ludmir EB, Desai V, Sved AF and Enquist LW. A dual infection pseudorabies virus conditional reporter approach to identify projections to collateralized neurons in complex neural circuits. PLoS One. 2011; 6:e21141.

53. Bariohay B, Roux J, Tardivel C, Trouslard J, Jean A and Lebrun B. Brain-derived neurotrophic factor/tropomyosin-related kinase receptor type B signaling is a downstream effector of the brainstem melanocortin system in food intake control. Endocrinology. 2009; 150:2646-2653.

54. Ye ZY and Li DP. Activation of the melanocortin-4 receptor causes enhanced excitation in presympathetic paraventricular neurons in obese Zucker rats. Regul Pept. 2011; 166:112-120.

55. Sohn JW, Xu Y, Jones JE, Wickman K, Williams KW and Elmquist JK. Serotonin 2C receptor activates a distinct population of arcuate pro-opiomelanocortin neurons *via* TRPC channels. Neuron. 2011; 71:488-497.

56. Zhou L, Sutton GM, Rochford JJ, Semple RK, Lam DD, Oksanen LJ, Thornton-Jones ZD, Clifton PG, Yueh CY, Evans ML, McCrimmon RJ, Elmquist JK, Butler AA, et al. Serotonin 2C receptor agonists improve type 2 diabetes *via* melanocortin-4 receptor signaling pathways. Cell Metab. 2007; 6:398-405.

57. Gautron L, Lee C, Funahashi H, Friedman J, Lee S and Elmquist J. Melanocortin-4 receptor expression in a vago-vagal circuitry involved in postprandial functions. J Comp Neurol. 2010; 518:6-24.

58. Ye DW, Liu C, Tian XB and Xiang HB. Identification of neuroanatomic circuits from spinal cord to stomach in mouse: retrograde transneuronal viral tracing study. International journal of clinical and experimental pathology. 2014; 7:5343-5347.

59. Ye D, Guo Q, Feng J, Liu C, Yang H, Gao F, Zhou W, Zhou L, Xiang H and Li R. Laterodorsal tegmentum and pedunculopontine tegmental nucleus circuits regulate renal functions: Neuroanatomical evidence in mice models. Journal of Huazhong University of Science and Technology Medical sciences. 2012; 32:216-220.

60. Ye DW, Li RC, Wu W, Liu C, Ni D, Huang QB, Ma X, Li HZ, Yang H, Xiang HB and Zhang X. Role of spinal cord in regulating mouse kidney: a virally mediated trans-synaptic tracing study. Urology. 2012; 79:745 e741-744.

61. Barker JR, Thomas CF and Behan M. Serotonergic projections from the caudal raphe nuclei to the hypoglossal nucleus in male and female rats. Respir Physiol Neurobiol. 2009; 165:175-184.

62. Franklin KB and Paxinos G. The mouse brain in stereotaxic coordinates. Third edition. San diego, CA: Academic press. 2007.

63. Molander C and Grant G. Spinal cord cytoarchitecture. In g. Paxinos(ed), the nervous system. Second edition. San diego, CA: Academic press. 1995.